Superparamagnetic Silica Composite Nanospheres (SSCNs) with Ultrahigh Loading of Iron Oxide Nanoparticles via an Oil-in-DEG Microemulsion Route

Ling Li, Eugene S. G. Choo, Jiabao Yi, Jun Ding, Xiaosheng Tang, and Junmin Xue*

Department of Materials Science and Engineering, National University of Singapore, Singapore 117576, Republic of Singapore

Received May 7, 2008
Revised Manuscript Received August 25, 2008

Composite nanospheres containing superparamagnetic iron oxide nanoparticles (SPIONs), either Fe_3O_4 or γ-Fe_2O_3, have been extensively studied for biological and environmental applications, such as the separation of various biological species and removal of contaminants from water.[1] The silica-based composite nanospheres is of particular interest because of its biocompatibity, stability against degradation, and simple prepapration procedure.[2] Moreover, the silica surface can be further modified with a wide range of functional groups.[2c] By the incorporation of other types of materials, such as quantum dots or gold nanoparticles, the magnetic nanospheres can be multifunctional.[3] However, a common problem encountered when applying these superparamagnetic silica composite nanospheres (SSCNs) is their poor magnetic response due to the low loading density of SPIONs, which makes the recovery of SSCNs much more time-consuming and even impractical.[4]

To date, there have been generally three main techniques that can be employed for fabricating SSCNs: aerosol pyrolysis, Stöber sol−gel, and water-in-oil reverse microemulsion methods. The aerosol pyrolysis method involves a mixture of silica and iron precursors.[5] Flame combustion is used to decompose the precursors, resulting in the formation of composite particles consisting of iron oxide and silica. A relatively high iron oxide loading density in the silica matrix can be achieved by using this method. However, this method requires high-temperature treatment (~500 °C), which might lead to aggregation of the resultant composite spheres. The Stöber sol−gel method was specifically designed for coating individual SPIONs with silica.[2a,6] The resultant core−shell nanoparticles also have generally low loading densities because of the thick shell.[6] Moreover, prior surface modification before silica coating is usually required to ensure a better silica shell.[7] One possibility of fabricating SSCNs with high SPION loading density through the Stöber method is to replace the discrete SPIONs with robust iron oxide clusters synthesized through a one-step solvothermal method.[8] However, the solvothermal conditions must be carefully adjusted to ensure the superparamagnetic performance of the resultant magnetic spheres.[1a] SPION clusters with well-defined superparamagnetic behavior, formed by bottom-up assembly routes,[9] may also serve as nuclei in the Stöber method, provided that they possess sufficient mechanical strength to withstand the mechanical stirring disturbance during the subsequent coating process.

Another technique for fabricating SSCNs is based on a reverse microemulsion technique. In this method, the loading density of SPIONs is determined by the amount of hydrophilic SPIONs dispersed in water droplets.[2c,10] The concentration of SPIONs in water droplets can be high, provided that the hydrophilic SPIONs are well dispersed and suspended in water even at high concentrations. However, as compared to the hydrophobic SPIONs, the preparation of high-quality, hydrophilic SPIONs is still a big challenge, although several techniques have been developed for fabricating hydrophilic SPIONs recently.[11] Because of the lack of high-quality, hydrophilic SPIONs, the SPION concentration has to be kept low, to achieve a stable reverse microemulsion system. Hydrophobic nanoparticles have also been tried in this reverse microemulsion method.[2c,12] The hydrophobic nanoparticles used are supposed to transfer into the hydrophilic interior through a rapid ligand exchange.[12] This modified process has yet to show a substantial increase

* Corresponding author. Tel: +65-6516 4655. Fax: +65 6776 3604. E-mail: msexuejm@nus.edu.sg.

(1) (a) Deng, Y.; Qi, D.; Deng, C.; Zhang, X.; Zhao, D. *J. Am. Chem. Soc.* **2008**, *130*, 28–29. (b) Lee, J.; Lee, Y.; Youn, J. K.; Na, H. B.; Yu, T.; Kim, H.; Lee, S.-M.; Koo, Y.-M.; Kwak, J. H.; Park, H. G.; Chang, H. N.; Hwang, M.; Park, J.-G.; Kim, J.; Hyeon, T. *Small* **2008**, *4*, 143–152. (c) Wang, Y.; Ng, Y. W.; Chen, Y.; Shuter, B.; Yi, J.; Ding, J.; Wang, S.; Feng, S.-S. *Adv. Funct. Mater* **2008**, *18*, 308–318.

(2) (a) Lu, Y.; Ying, Y. D.; Mayers, B. T.; Xia, Y. N. *Nano Lett.* **2002**, *2*, 183. (b) Selvan, S. T.; Tan, T. T.; Ying, J. Y. *Adv. Mater.* **2005**, *17*, 1620–1625. (c) Yi, D. K.; Selvan, T.; Lee, S. S.; Papaefthymiou, G. C.; Kundaliya, D.; Ying, J. Y. *J. Am. Chem. Soc.* **2005**, *127*, 4990.

(3) (a) Li, L.; Choo, E. S. G.; Liu, Z.; Ding, J.; Xue, J. *Chem. Phys. Lett.* **2008**, *461*, 114–117. (b) Insin, N.; Tracy, J. B.; Lee, H.; Zimmer, J. P.; Westervelt, R. M.; Bawendi, M. G. *ACS Nano* **2008**, *2*, 197–202. (c) Ge, J.; Huynh, T.; Hu, Y.; Yin, Y. *Nano Lett.* **2008**, *8*, 931–934.

(4) Jeong, U.; Teng, X.; Wang, Y.; Yang, H.; Xia, Y. *Adv. Mater.* **2007**, *19*, 33–60.

(5) (a) Tartaj, P.; Serna, C. J. *J. Am. Chem. Soc.* **2003**, *125*, 15754–15755. (b) Tartaj, P.; Gonziález-Carreño, T.; Ferrer, M. L.; Serna, C. J. *Angew. Chem., Int. Ed.* **2004**, *43*, 6304–6307.

(6) Deng, Y.-H.; Wang, C.-C.; Hu, J.-H.; Yang, W.-L.; Fu, S.-K. *Colloids Surf. A* **2005**, *262*, 87–93.

(7) (a) Graf, C.; Vossen, D. L. J.; Imhof, A.; van Blaaderen, A. *Langmuir* **2003**, *19*, 6693–6700. (b) Graf, C.; Dembski, S.; Hofmann, A.; Rühl, E. *Langmuir* **2006**, *22*, 5604–5610.

(8) Ge, J.; Hu, Y.; Biasini, M.; Beyermann, W. P.; Yin, Y. *Angew. Chem., Int. Ed.* **2007**, *46*, 4342–4345.

(9) (a) Bai, F.; Wang, D.; Huo, Z.; Chen, W.; Liu, L.; Liang, X.; Chen, C.; Wang, X.; Peng, Q.; Li, Y. *Angew. Chem., Int. Ed.* **2007**, *46*, 6650–6653. (b) Zhuang, J.; Wu, H.; Yang, Y.; Cao, Y. C. *J. Am. Chem. Soc.* **2007**, *129*, 14166–14167.

(10) (a) Yang, Y. H.; Gao, M. *Adv. Mater.* **2005**, *17*, 2354–2357. (b) Yang, Y.; Jing, L.; Yu, X.; Yan, D.; Gao, M. *Chem. Mater.* **2007**, *19*, 4123–4128. (c) Stierndahl, M.; Andersson, M.; Hall, H. E.; Pajerowski, D. M.; Meisel, M. W.; Duran, R. S. *Langmuir* **2008**, *24*, 3532–3536. (d) He, R.; You, X.; Shao, J.; Gao, F.; Pan, B.; Cui, D. *Nanotechnology* **2007**, *18*, 315601.

(11) (a) Ge, J. P.; Hu, Y. X.; Biasini, M.; Dong, C. L.; Guo, J. H.; Beyermann, W. P.; Yin, Y. D. *Chem.—Eur. J.* **2007**, *13*, 7153. (b) Li, Z.; Wei, L.; Gao, M.; Lei, H. *Adv. Mater.* **2005**, *17*, 1001–1005. (c) Wan, J.; Cai, W.; Meng, X.; Liu, E. *Chem. Commun.* **2007**, 5004–5006.

(12) Koole, R.; van Schooneveld, M. M.; Hilhorst, J.; de Mello Donegá, C.; C't Hart, D.; van Blaaderen, A.; Vanmaekelbergh, D.; Meijerink, A. *Chem. Mater.* **2008**, *20*, 2503.

10.1021/cm8012107 CCC: $40.75
Published on Web 10/01/2008

Scheme 1. Formation of SSCNs via an Oil-in-DEG Route

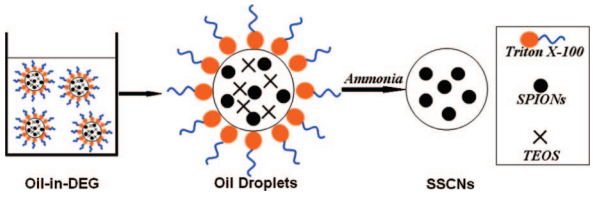

in the loading density due to the poor efficiency of the polarity transfer. Normally, the magnetization of the SSCNs derived from the reverse microemulsion is <5 emu/g, which is much smaller than the magnetization of pure SPIONs (40−60 emu/g for Fe_3O_4).

In this work, we report a new strategy of a silica coating technique with the aim of fabricating SSCNs with an ultrahigh loading density of SPIONs. This method is based on a unique oil-in-DEG (diethylene glycol) micromulsion system, as illustrated in Scheme 1. Generally, hydrophobic SPIONs and tetraethylorthosilicate (TEOS) are entrapped in oil droplets that are stabilized in DEG by the surfactant, forming a stable oil-in-DEG microemulsion. The hydrolysis and condensation of TEOS occurs within the oil droplets after the added ammonia diffuses through DEG. This oil-in-DEG technique offers the following advantages over the conventional silica coating techniques: (1) Hydrophobic SPIONs are used instead of hydrophilic SPIONs, and no prior surface modification is requried. These hydrophobic particles have superb colloidal stability and can be easily reproduced,[13] which will lead to a high loading amount of SPIONs in oil droplets. (2) TEOS is constrained in oil droplets together with SPIONs, ensuring that the hydrolysis and condensation reactions only occur in the oil droplets in the presence of SPIONs, avoiding the formation of empty silica spheres. (3) DEG is used as the polar medium instead of water. The clever use of DEG effectively limits the hydrolysis and condensation of TEOS within the oil droplets, resulting in better control of the particle size and avoidance of agglomeration.

Hydrophobic SPIONs with an average particle size of 6.6 nm are prepared according to a previous report[13a] and are then used for the synthesis of SSCNs (Figure S1 in the Supporting Information). Three SSCN samples with different loading rates of SPIONs, namely, SSCN-01, -02, and -03, are prepared through the oil-in-DEG route. The loading rates are modified by adjusting the concentration of SPIONs in the oil phase. Figure 1a is a typical field-emission scanning electron microscopy (FESEM) image of SSCN-01. Well-defined spherical nanospheres with an average particle size of 300 nm are obtained, and no aggregation among the particles is observed. The particles can be easily aligned during the drying process when a magnetic field is applied (Figure S4 in the Supporting Information). This demonstrates the high magnetization of the as-synthesized composite spheres, which can be easily manipulated by an external magnetic field. Figure 1b, a typical transmission electron

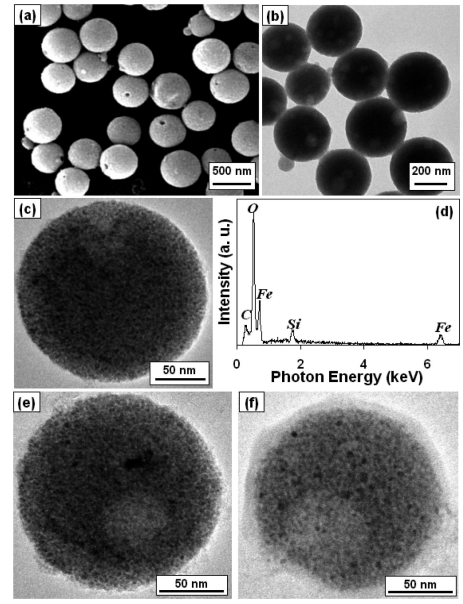

Figure 1. (a) FESEM and (b) TEM images of SSCN-01. (c) TEM image of a typical SSCN-01 nanosphere. (d) EDX analysis of SSCN-01, demonstrating the coexistence of silica and iron oxide in the composite nanospheres. (e and f) TEM images of SSCN-02 and -03, respectively.

microscopy (TEM) image of Figure S1 in the Supporting Information, confirms the successful incorporation of SPIONs in the composite nanospheres. Figure 1c is the TEM image of a single typical SSCN. Densely packed SPIONs are clearly observed in the amorphous silica matrix. A smooth surface can be observed, and no particles reside at the surface of the composite nanospheres. Moreover, individual SPIONs can be seen by carefully focusing at the edge of a nanosphere (Figure S5 in the Supporting Information). The presence of iron oxide in the nanosphere is also verified by energy-dispersive X-ray (EDX) analysis, as shown in Figure 1d. The product is further studied through Fourier transform infrared spectroscopy (Figure S6 in the Supporting Information). It can be clearly seen that the absorption band at ~640 cm^{-1}, corresponding to the Fe−O bond,[13b] appears for both SPIONs and SSCNs. Moreover, the siloxane (Si−O−Si) band appears as a broad strong peak centered at 1100 cm^{-1}, which confirms the formation of a silica matrix.[14a] Another new adsorption band at 1630 cm^{-1} for SSCNs is due to the deformation vibrations of adsorbed water molecules,[14b] which is not observed for pure SPIONs because of their hydrophobic nature. One of the advantages of this oil-in-DEG route to synthesize SPION-incorporated nanospheres is that the loading density of the SCCNs can be easily controlled by adjusting the concentration of SPIONs in the oil phase. SSCN-02 and -03, with lower loading rates of SPIONs by decreasing the concentration of SPIONs in the oil phase, are synthesized, and typical TEM images are shown in parts e and f of Figure 1, respectively.

In addition, it was noticed that there are small defects at the surface of the as-synthesized SSCNs, as shown in Figure 1a. It is believed these defects are formed as a result of the presence of unreacted toluene in the microemulsion system. The unreacted toluene was vaporized during the subsequent drying process after synthesis, leading to the formation of voids or surface defects. A control experiment is conducted

(13) (a) Sun, S.; Zeng, H.; Robinson, D. B.; Raoux, S.; Rice, P. M.; Wang, S. X.; Li, G. *J. Am. Chem. Soc.* **2004**, *126*, 273. (b) Park, J.; An, K.; Hwang, Y.; Park, J.-G.; Noh, H.-J.; Kim, J.-Y.; Park, J.-H.; Hwang, N.-M.; Hyeon, T. *Nat. Mater.* **2004**, *3*, 891.

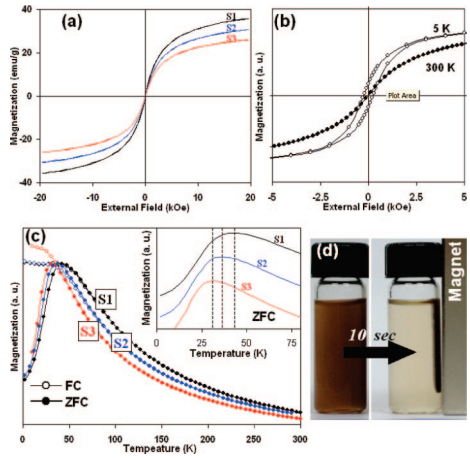

Figure 2. (a) Field-dependent magnetization plots of SSCN-01, -02, and -03 at room temperature. (b) Field-dependent magnetization plots of SSCN-01 at 300 and 5 K, respectively. (c) ZFC and FC curves of SSCN-01, -02, and -03 between 5 and 300 K. The inset in part c is a magnified view of the ZFC curves at low applied fields. (d) Photograph of SSCNs driven by an external magnet in water.

by completely eliminating the use of toluene in the oil phase, and SSCNs without any defects can be readily obtained (Figure S7 in the Supporting Information).

The magnetic properties of SSCN-01, -02, and -03 at 300 K are recorded using a vibrating sample magnetometer. Field-dependent magnetization plots show that all samples are superparamagnetic at 300 K (Figure 2a). The ferromagnetic property of the SSCN-01 sample at 5 K is further addressed using a superconducting quantum interference device (SQUID) (Figure 2b). The saturation magnetization (M_s) values of SSCN-01, -02, and -03 are measured to be 33.60, 28.98, and 24.36 emu/g at 300 K, respectively. By comparison with the M_s value of the pure SPIONs used (42 emu/g; Figure S2 in the Supporting Information), the loading rates of the three samples are estimated to be 80, 69, and 58 wt %, respectively. More accurately, the Fe_3O_4 loading of the SSCN-01 sample was measured by using ICP chemical analysis. The measured loading rate of Fe_3O_4 in the SSCN-01 sample was ~89 wt %, which is slightly higher than the estimated loading rate on the basis of magnetization. It is believed that the magnetization of the obtained SSCNs is also affected by the interaction between iron oxides and the silica matrix. This will lead to an underestimation of the actual iron oxide loading in SSCNs if the iron oxide loading rate is calculated on the basis of the magnetization measurement. Zero-field-cooled (ZFC) and field-cooled (FC) magnetization curves of three samples are registered under an applied field of 100 Oe between 5 and 300 K (Figure 2c). All of the samples exhibit superparamagnetic behavior, similar to that of pure SPIONs. The blocking temperature (T_B) of SSCN-01 is 42 K, which is 21 K higher compared with those of the pure SPIONs (Figure S3 in the Supporting Information). The shifting of T_B to a higher temperature can be attributed to the interaction between magnetic nanoparticles because of the agglomeration of SPIONs in SCCNs, which is highly possible because the loading rate of SPIONs in SSCNs is so high.[1c] In the oil-in-DEG microemulsion system, both TEOS and SPIONs are confined in the oil droplets. Hydrolysis and condensation of TEOS in these droplets result in the formation of the silica matrix. The difference in density between TEOS (0.93 g/cm^3) and silica (2.20 g/cm^3) leads to a substantial volume shrinkage, resulting in a high packing density of SPIONs. Therefore, the coupling interaction between SPIONs would require extra thermal energy to overcome the energy barrier, which results in the higher blocking temperature.[15] T_B of SSCN-02 and -03 are 37 and 30 K, respectively, which are expected because if the reduction in the SPION loading density as compared to that of SSCN-01.

Figure 2d demonstrates the magnetic manipulation ability of SSCNs dispersed in an aqueous solution. Nearly all of the dispersed nanospheres can be attracted by an external magnet within 10 s, showing a very strong magnetic response. The attracted nanospheres can be redispersed quickly with a mild shaking once the external magnet is removed.

In conclusion, we have developed a novel oil-in-DEG microemulsion route for the fabrication of superparamagnetic silica composite nanospheres with an ultrahigh loading density of SPIONs. The as-synthesized SCCNs exhibit a much higher saturation magnetization because of the high loading density of SPIONs compared to others reported in the current literature. The SCCNs possess well-defined superparamagnetism and demonstrate strong response to an external magnetic field, presenting us with an excellent tool for magnetic separation. Moreover, this newly developed silica coating technique can also be used as a highly versatile encapsulation technique for other hydrophobic nanoparticles, such as quantum dots.

Acknowledgment. This work is supported by the Singapore MOE's ARF Tier 1 funding WBS R-284-000-050-133.

Supporting Information Available: Enlarged Figures 1 and 2, detailed experimental and characterization procedures, characterizations of pure SPIONs, and supporting characterizations. This material is available free of charge via the Internet at http://pubs.acs.org.

CM8012107

(14) (a) Pérez-Quintanilla, D.; del Hierro, I.; Fajardo, M.; Sierra, I. *J. Mater. Chem.* **2006**, *16*, 1757–1764. (b) Pavia, D.; Lampman, G.; Kriz, G. *Introduction to Spectroscopy*; Harcourt College Publishers: Avenel, NJ, 2001.

(15) Lin, C. R.; Chiang, R. K.; Wang, J. S.; Sung, T. W. *J. Appl. Phys.* **2006**, *99*, 1.